



MINISTÉRIO DA CIÊNCIA E TECNOLOGIA
INSTITUTO NACIONAL DE PESQUISAS ESPACIAIS

INPE-11304-PRE/6741

**OVERVIEW OF RESEARCH ON AUTONOMOUS ORBIT
CONTROL AT INPE**

Valcir Orlando
Hélio Koiti Kuga

ADVANCES IN SPACE DYNAMICS 4: CELESTIAL MECHANICS AND ASTRONAUTICS,
H. K. Kuga, Editor, 253-268 (2004).
Instituto Nacional de Pesquisas Espaciais – INPE, São José dos Campos, SP, Brazil.
ISBN 85-17-00012-9

INPE
São José dos Campos
2004

OVERVIEW OF RESEARCH ON AUTONOMOUS ORBIT CONTROL AT INPE

Valcir Orlando

Hélio Koiti Kuga

INPE - Instituto Nacional de Pesquisas Espaciais

Avenida dos Astronautas, 1758 - J. da Granja, 12227-010 - São José dos Campos – SP

e-mail: valcir@ccs.inpe.br

ABSTRACT

An overview of the investigations carried out at INPE in the field of autonomous orbit control systems is presented and discussed. The first work consisted of an investigation on the feasibility of an autonomous control concept of the orbit longitude phase drift (ΔL_0), carried out in cooperation with the French Space Agency (CNES) in 1995. The use of a French navigator, called DIODE, was considered in order to provide the required real time orbit estimates. It computes estimates of the satellite position and velocity components, by processing the Doppler measurements generated by an on-board DORIS system receiver. Thereafter, the research work was directed to the investigation on the use of the GPS (Global Positioning System) instead of DIODE. At first, only the direct use of the coarse GPS navigation (geometric) solution was considered. In order to improve the results a GPS simplified navigator was further developed. The addition of such navigator to the autonomous orbit control significantly reduced the variation range of ΔL_0 . Samples of the results obtained in each phase of the performed investigation are presented and commented.

INTRODUCTION

With the advent of the modern positioning systems, like GPS and DORIS (Putney and al, 1992; Nouel et al, 1993) for instance, reliable and accurate autonomous navigation means are being more and more developed and explored. The generated on-board availability of continuous and accurate knowledge of the satellite orbit, makes feasible the idea of increasing the autonomy of orbit control processes. Particularly attractive is the case of having autonomous control of the longitude phase drift, ΔL_0 , for phased earth observation satellites, in order to assure the repeatability of the orbit ground track, since, for this kind of mission, this is the parameter that requires the higher corrective maneuver rate.

The first INPE's work related to autonomous orbit control took place in 1995, when a study on the feasibility of an autonomous control concept of ΔL_0 was performed, in cooperation with the French Space Agency (CNES) (Orlando and Micheau, 1996). Real and simulated orbit estimates from DIODE navigator (Berthias and al, 1993; Tournier and al, 1999) were, then, considered. Three versions of autonomous orbit control procedures have been studied. The first one computes the orbit

correction amplitudes with help of a simplified parabolic model for the longitude drift time evolution, whose parameters are estimated in real time. The second one always applies orbit corrections with a constant amplitude, independently of the current conditions in terms of navigation error magnitude and solar activity. Finally, in the third version, the corrections amplitude are taken as a function of the current solar activity conditions, inferred from estimates of $\ddot{\Delta L}_0$. The feasibility of improving the autonomous orbit control performance by reducing the oscillations in the observations of $\dot{\Delta L}_0$ caused by the geopotential tesseral harmonics (Orlando and al, 1997) was also analyzed.

Thereafter, following a world wide trend, the study was directed to the investigation on the use of the GPS (Global Positioning System) instead of DIODE (Orlando and Kuga, 1999). At first, the direct use of the coarse GPS navigation (geometric) solution was considered (Gill, 1997; Hart and al, 1997). This GPS solution presents which are several orders of magnitude greater than the ones presented by DIODE. Concluding this analysis, an study of the influence of the maximal allowable maneuver application rate was performed (Orlando and Kuga, 2000).

The next step consisted of the development of a simplified GPS navigator, in order to improve the accuracy of the GPS geometrical navigation solution. It consists of a Kalman filtering process, which uses the position components of the GPS navigation solution as observations, and incorporates a procedure for automatic treatment of observation biases. Its inclusion to the autonomous orbit control procedure [Galski and al, 2002] do not added a significant computational burden to the overall process, but allowed to obtain a significant reduction in the variation range of ΔL_0 .

The autonomous control concept is described in the next section. Thereafter the main aspects of the preliminary study performed by INPE regarding this subject are presented and commented. After that, the performed feasibility analysis of directly applying the GPS navigation solution in the autonomous orbit control, is summarized. Following this, a new section presents and discusses the relevant results related to the development of the above mentioned simplified GPS navigator, and its application to autonomous orbit control. Finally, some comments and conclusions are presented in a final section.

AUTONOMOUS CONTROL PROCEDURE

General Description

The general block diagram of the autonomous control system is presented in Fig. 1.

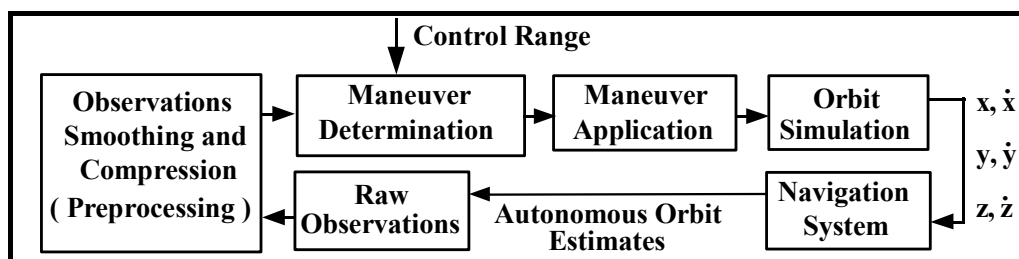


Fig. 1. Block Diagram for the autonomous orbit control system

The first task is the computation of raw observations of ΔL_0 and $\dot{\Delta L}_0$ from the orbit estimates issued by the navigator. The following equations are used in this task (Orlando,1999):

$$\Delta L_0 = a_e \cdot \left[\Delta \Omega + \frac{\Delta \alpha}{(N + P/Q)} \right] \quad (1)$$

$$\dot{\Delta L}_0 = -\frac{3\pi}{T_{te}} \left(\frac{a_e}{a_R} \right) (1 - \varepsilon) \left[\Delta a - \left(\frac{da}{di} \right)_p \Delta i \right], \quad (2)$$

where T_{te} is the mean solar day; a_e is the Equator radius, a_R is the reference orbit semi major axis;

$$\varepsilon = \frac{7}{3} \frac{T_{te}}{T_{so}} + \frac{7}{2} J_2 \left(\frac{a_e}{a} \right)^2 [4 \cos^2(i) - 1]; \quad \text{and} \quad \left(\frac{da}{di} \right)_p = -\frac{2}{3} a \tan(i) \frac{T_{te}}{T_{so}} \frac{(1 + \eta)}{(1 + \varepsilon)}; \quad (3)$$

where: $T_{so} = 1$ year and $\eta = 12 J_2 (T_{so}/T_{te}) (a_e/a)^2 \cos^2(i)$.

It is assumed constant solar flux during the time interval between the application of two successive orbit correction maneuvers, which implies in having constant da/dt (a being the orbit semi-major axis) during this interval. Under this assumption, the time evolution curve of ΔL_0 is almost parabolic, and (calling $\Delta t = t - t_0$) can be modeled by:

$$\Delta L_0(t) = \Delta L_0(t_0) + \dot{\Delta L}_0(t_0) \Delta t + \ddot{\Delta L}_0(t_0) \Delta t^2 / 2 \quad (4)$$

From this equation, the first time derivative of ΔL_0 , $\dot{\Delta L}_0(t)$, can be written as:

$$\dot{\Delta L}_0(t) = \dot{\Delta L}_0(t_0) + \ddot{\Delta L}_0(t_0) \Delta t \quad (5)$$

The computed raw observations of $\dot{\Delta L}_0(t)$ are preprocessed in real time, in order to achieve data smoothing by curve fitting, validation and redundancy reduction. The preprocessed values are used as

observation, by a Kaman filtering process which provides real time estimates of $\hat{\Delta L}_0(t_k)$ and $\hat{\dot{\Delta L}}_0(t_k)$, $k=1, 2, \dots$. Estimates of the remaining coefficient, of Equation 4 ($\Delta L_0(t_k)$) are computed from:

$$\hat{\Delta L}_0(t_k) = [\sum_{i=0}^{k-1} p_i \overline{\Delta L_0(t_i)} + p_k \overline{\Delta L_0(t_k)}] / (\sum_{i=0}^{k-1} p_i + p_k) \quad (6)$$

where p_0, p_1, \dots, p_k are weighting factors.

The estimates $\hat{\Delta L}_0(t_k)$, $\hat{\dot{\Delta L}}_0(t_k)$ and $\hat{\ddot{\Delta L}}_0(t_k)$ are used by the block “Maneuver Determination and Computation” to determine the need of maneuvers and to compute the required correction amplitudes. In order to test the autonomous control procedure, the control loop is closed with help of a realistic orbit simulator, from whose outputs the navigator orbit estimates are simulated.

Determination of Maneuver Needs

The following three versions of the autonomous control procedure have been studied:

- a** - Variable Amplitude Corrections
- b** - Constant Amplitude Corrections.
- c** - Adaptive Amplitude Corrections.

Both procedures consider the same process of determining the need of maneuver applications. Due to orbital decay the satellite ground track drifts Eastward. One semi-major axis increment is assumed to be needed to correct the time evolution of ΔL_0 each time the two conditions below are both satisfied:

$$\hat{\Delta L}_0(t_k) > \Delta L_{0sup} - n \cdot \sigma(t_k), \quad \text{and} \quad \hat{\dot{\Delta L}}_0(t_k) > \dot{\Delta L}_{0sup} + n_p \cdot \sigma_p(t_k), \quad (7)$$

where ΔL_{0sup} and $\dot{\Delta L}_{0sup}$ are previously chosen control limit values; $\sigma(t_k)$ and $\sigma_p(t_k)$ are the standard deviations of $\hat{\Delta L}_0(t_k)$ and $\dot{\hat{\Delta L}}_0(t_k)$ and n and n_p are two previously chosen real numbers.

Variable Amplitude Corrections

This version computes each orbit correction so as to cause a change in the sense of $L_0(t)$ in such a way that the minimum value to be attained, considering the parabolic model of Equation 4, will be equal the previously chosen lower limit of control. In order to maximize the time interval between the execution of two successive maneuvers, only positive semi-major axis correction is allowed to be applied. The Fig. 2 illustrates the procedure used for computing the corrections amplitude:

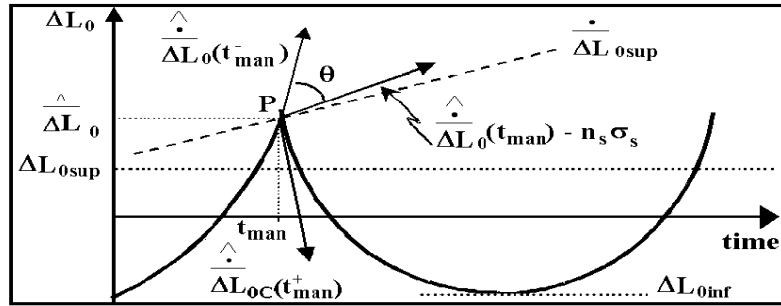


Fig.2. Maneuver calculation

This figure shows the almost parabolic time evolution curve of ΔL_0 . It is supposed that at the instant $t = t_{man}$ the application of one semi major axis increment maneuver is verified to be needed. This maneuver shall be calculated such that it causes a change in the value of $\dot{\Delta L}_0$, so that the minimal value to be attained by ΔL_0 be equal to a previously chosen inferior limit of control, as illustrated in Fig.2. This strategy implies in the maximization of the time interval between two successive maneuvers. The predicted evolution of ΔL_0 after any maneuver execution can be written as:

$$\hat{\Delta L}_0(t/t_{man}) = \hat{\Delta L}_0(t_{man}/t_{man}) + \dot{\Delta L}_{0c}(\Delta t_{man}^+) \Delta t_{man} + \frac{1}{2} \ddot{\Delta L}_0(t_{man}/t_{man}) \Delta t_{man}^2 \quad (8)$$

where: $\dot{\Delta L}_{0c}(t_{man}^+)$ is the wanted value for $\dot{\Delta L}_0$ just after the maneuver application and $\Delta t_{man} = t - t_{man}$.

Calculating the value of $\dot{\Delta L}_{0c}(t_{man}^+)$ so that the minimum value to be attained by $\hat{\Delta L}_0(t/t_{man})$ be equal to a pre-specified inferior control limit, ΔL_{0inf} , one obtain:

$$\dot{\Delta L}_{0c} = \sqrt{2 \cdot \dot{\Delta L}_0(t_{man}) \cdot [\dot{\Delta L}_0(t_{man}) - \Delta L_{0inf}]} \quad (9)$$

This implies, of course, that $\ddot{\Delta L}_0$ be positive (natural Eastwards longitude drift). For phased heliosynchronous orbits one can write the differential equation relating the longitude phase drift to the orbit semi-major axis and inclination as (Micheau, 1995):

$$\ddot{\Delta L}_0(t) = - \left(\frac{3\pi a_e}{T_{te} \cdot a_R} \right) (1 + \varepsilon) \left[\frac{da}{dt} - \left(\frac{da}{di} \right)_P \frac{di}{dt} \right] \quad (10)$$

If one takes the approximation $1 + \varepsilon \cong 1$ and considering that at CBERS1 like altitudes the atmospheric drag is the dominant perturbing force over the satellite orbit, one can neglect the dependence of ΔL_0 on the orbit inclination. Under this assumption the equation 10 can be written as:

$$\ddot{\Delta L}_0(t) = -\frac{3\pi}{T_{te}} \frac{a_e}{a} \frac{da}{dt} \quad (11)$$

Supposing that the value of $\frac{da}{dt}$ is constant during the time interval involved between two successive maneuvers, one can easily arrive at the following equation for computing the tangential velocity increments to be imposed to the orbit, in order to correct the time evolution of ΔL_0 :

$$\Delta v_T = -\frac{T_{te} \cdot V \cdot [\overset{\wedge}{\Delta L}_{oc} - \overset{\wedge}{\Delta L}_0(t_{man}/t_{man})]}{6\pi \cdot a_e} \quad (12)$$

where V is the absolute value of the satellite speed. This equation is utilized to compute Δv_T by the variable amplitude corrections version of autonomous orbit control procedure. Whenever one orbit correction is applied to the satellite, the coefficient estimation procedure, mentioned above, is automatically re-initialized in order to avoid filter divergence.

Constant Amplitude Corrections

The Constant Amplitude Corrections version does not perform any computation of orbit correction amplitude. It has always the same value, independently of the current conditions in terms of navigation error magnitude and solar activity. Each time the conditions given by Equations 7 are both satisfied one semi-major axis increment with constant amplitude, are applied to correct the time

evolution of ΔL_0 . This strategy may be interesting if $\overset{\wedge}{\ddot{\Delta L}}(t)$ is no more considered as constant, i.e. for higher altitudes (when di/dt becomes significant), or for strong variations of atmospheric drag (da/dt not constant).

The correction amplitude must be chosen small enough so that the minimum value reached by ΔL_0 be greater than the inferior control limit, even in periods of minimal solar activity. On the other hand, the maximal allowed orbit correction rate must be great enough in order that the control action can produce an inversion in the ΔL_0 time derivative when under important solar activity level. If one wants to reduce the control limits, maintaining however similar performance characteristics, under any solar activity condition, then it will be necessary to reduce the correction amplitude for the constant corrections and, in addition, to increase the maximal allowed rate of its application. Depending on the desired control range, getting a satisfactory performance of this kind of procedure can imply having prohibitively small amplitudes of correction and/or prohibitively high correction application rates.

Adaptive Amplitude Corrections

In order to try to avoid the above mentioned problems which can occur with the Constant Correction Amplitude version, the introduction of an improvement on it was considered: This basically consists in always applying a previously chosen value of the corrections amplitude, while the solar activity remains inside an fixed range. When the solar activity goes outside this range, then a new constant value is considered for the corrections amplitude, but only while the solar activity remains inside to

another adjacent range, and so on. In other words, each correction amplitude is automatically chosen as a function of the current conditions in terms of solar activity. For this purpose solar activity is divided in several variation ranges, and one single value of orbit correction amplitude is previously associated to each one of these ranges. When the application of an orbit correction is verified to be needed, the control procedure autonomously selects the correction amplitude which corresponds to the current solar activity condition. The problem imposed to the application of this approach is that the instantaneous values of the solar flux are not available on-board of the satellite. Fortunately, its magnitude can, however, be inferred from the estimates of the second time derivative of ΔL_0 , that is, $\frac{\ddot{\Delta L}_0}{\Delta L_0}(t)$, which is naturally computed by the autonomous control procedure, with help of the before mentioned Kalman filtering procedure. Actually, in the performed analysis, only three discrete values of semi major axis corrections were considered is the current analysis, that is:

$$\Delta a = A1 \text{ m if } \frac{\overset{\wedge}{\ddot{\Delta L}}}{\Delta L}(t_{k-1}/t_{k-1}) < L1 \text{ m/s}^2, \quad (13)$$

$$\Delta a = A2 \text{ m if } L1 \text{ m/s}^2 \leq \frac{\overset{\wedge}{\ddot{\Delta L}}}{\Delta L}(t_{k-1}/t_{k-1}) \leq L2 \text{ m/s}^2, \quad (14)$$

$$\Delta a = A3 \text{ m if } \frac{\overset{\wedge}{\ddot{\Delta L}}}{\Delta L}(t_{k-1}/t_{k-1}) > L2 \text{ m/s}^2, \quad (15)$$

where: A1, A2 and A3 are the chosen correction amplitudes, and L1 and L2 are limit values of $\frac{\overset{\wedge}{\ddot{\Delta L}}}{\Delta L}$.

PRELIMINARY STUDIES

In the preliminary studies, both real and simulated from a DIODE like navigator were used to perform the tests on the autonomous control concept. The orbit estimates was simulated at a rate of 1 set each 10 seconds, with rms errors of 10m in the position and 0.001 m/s in the velocity components of the state vector. The performance of the proposed autonomous control was analyzed over a simulation period of about one year, considering worst conditions in terms of solar activity variation, as it can be seen by Fig. 3. The solar flux 11-year cycle has been shortened into one year simulation, with a very high maximum (360 in flux units), and kept the 27-day cycle oscillations due to solar rotation.

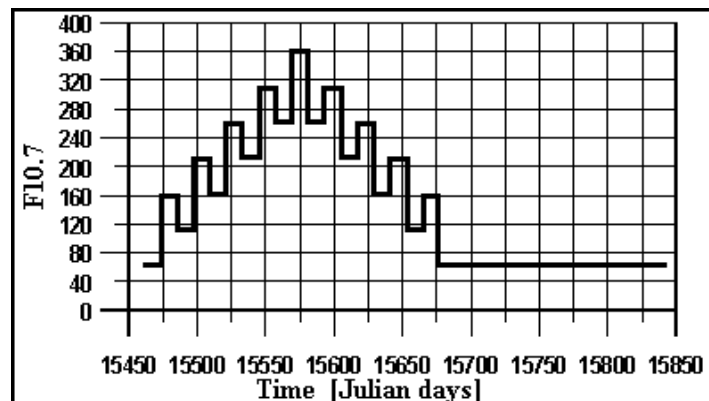


Fig. 3. Solar Flux

The Fig.4 shows the best preliminary results which have been obtained for the Variable Amplitude Corrections version of the autonomous orbit control procedure, when no tesseral effect correction is

applied. DIODE like estimates were simulated with standard deviation of 30m in the position components of the orbit state vector, and 0.01m/s in the velocity ones. One can see from Fig. 4 that the longitude phase drift remained inside a restrict range of about -200 to 400m. This result was very promising, since for SPOT2 and SPOT3, as instance, this parameter should nominally be maintained inside the range of ± 3000 m, and inside ± 10000 m, for CBERS1.

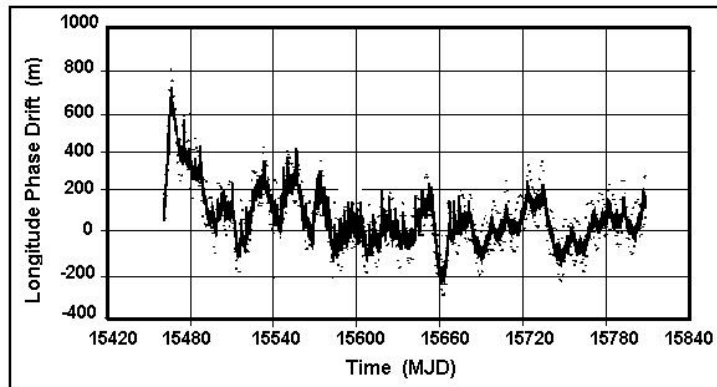


Fig. 4. ΔL_0 vs time : Variable Amplitude Corrections

The Fig. 5 shows the best result obtained when the constant amplitude corrections was considered. In this case Δa has been taken equal to 8m. One can observe that the curve of ΔL_0 presents an increasing trend, when the solar activity is high. On the other hand, under low solar activity negative deviations occurred. This means that, with the considered maximal maneuver rate (1 correction per orbit) the correction amplitude is not large enough to reduce the error, when under strong solar activity. On the other hand, when solar activity is weak, the chosen correction amplitude shows to be excessively large.

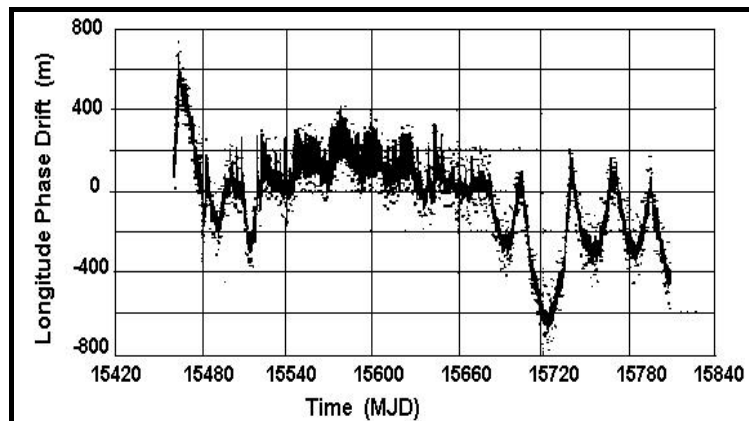


Fig. 5. ΔL_0 vs time: Constant Amplitude Corrections

This situation should be avoided by the use of the adaptive amplitude corrections procedure which consists of an improved version of the previous one. The Fig. 6 presents the results obtained when this procedure version was applied to the same test case above. Comparing the curves of Fig 6 and Fig. 5 one observes, besides a reduction in the ΔL_0 variation, the absence of the above mentioned problems presented by the constant amplitude corrections version.

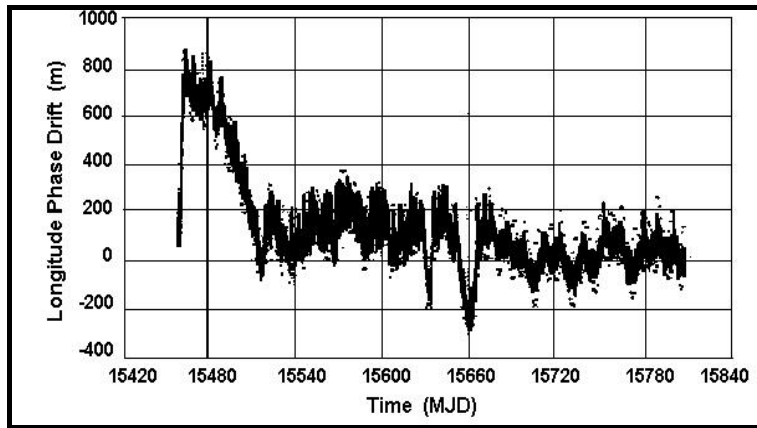


Fig. 6. ΔL_0 vs time: Adaptive Amplitude Corrections

Further, the influence in the observations of $\dot{\Delta L}_0$ of correction for the effects of the geopotential tesseral harmonics on the orbit inclination was analyzed. A revised issue of the Ustinov's theory for near circular orbits, taken tesseral terms up to J_{44} , was considered (Eckstein and Hechler, 1970) in a simplified form, by assuming the approximations: $\sin(i) \cong 1$ ($i \cong 90^\circ$) and $T_{te}/T_{sa} \ll 1$. After the tesseral effects correction, the curve of ΔL_0 remained restricted to a reduced variation range of about ± 200 m

USE OF THE GPS NAVIGATION SOLUTION

Thereafter, following a world wide trend, the study was directed to the use of the GPS (Global Positioning System) instead of DIODE. At first, the aim of the study was the analysis of the feasibility of straightforward application of the GPS coarse navigation solution in the autonomous orbit control process. This GPS solution is several order of magnitude less accurate than the ones issued by DIODE. Typical root mean square errors of the coarse GPS estimates were of 100m in position and 1m/s in velocity, before Selective Availability was turned off. Added to such random errors these estimates showed systematic variations with values of the order of 100m and duration of about 1 to 15 minutes. They occur due to the changes of the set of GPS satellites which are visible to the on-board GPS receiver. Each GPS satellite has its own systematic error and, each time a satellite goes out of the GPS receiver antenna coverage region, or a new satellite enters in this region, the systematic error is prone to change its value. The GPS coarse navigation solution was simulated by the addition of a gaussian white noise to the orbit state vector components. The Fig. 7 presents the results obtained by the application of the constant amplitude corrections version of the autonomous control procedure.

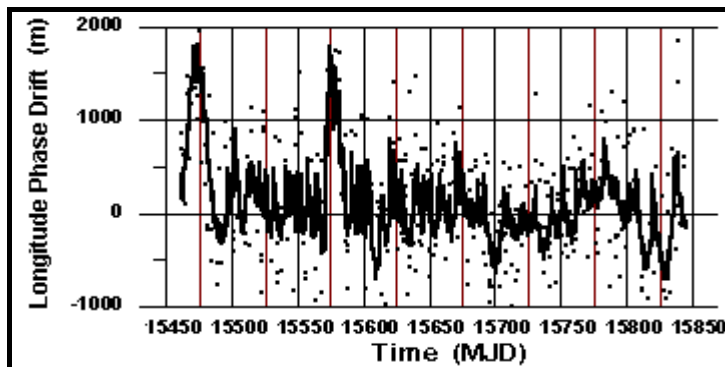


Fig. 7. ΔL_0 vs time: Constant Amplitude Corrections (GPS)

One can see that, as expected, the control range is increased when the GPS navigation solution replaces the more accurate DIODE like orbit estimates. Anyway, the control procedure successfully maintains the values of ΔL_0 under control during all simulated interval (about 1 year), even under the very severe solar flux conditions considered in the simulation. This enlarged control range (of about -1000m to 1700m, as seen by Fig. 7) was, however, satisfactory, since the nominal variation range of ΔL_0 specified for, for some existing phased Earth observation satellites, are larger than it (10,000m in the case of CBERS1, for instance). These results 5 are a little better than the ones that have been obtained, in the same case, with the application of the procedure version of variable correction amplitudes. As the constant amplitude corrections version does not compute the amplitude of correction, it does not face the risk of computing values of correction which are excessively large or small. The orbit corrections have always the same amplitude but, depending on the current conditions in terms of solar activity, the correction applications rate are automatically increased or decreased. Due to this feature, this version of the autonomous orbit control procedure presents higher robustness characteristics than the variable amplitude corrections one.

Analysis of the Maximal Allowable Maneuver Application Rate

The results presented in previous sections considered a very high sampling rate of the GPS orbit estimates: 1 estimate set every 10 seconds. In addition, a very high maximal allowable application rate of one semi-major axis correction per orbit period was assumed. Due to this, a further analysis of the influence of the maximal allowable maneuver application rate on the performance of the autonomous control procedure has been developed. This analysis has been carried out considering the application of the procedure version which considers adaptive corrections amplitude. Actually, such version was the one that presented the best performance among all the ones analyzed in previous studies. The same worst case conditions, in terms of solar activity assumed in the previous investigations, have been considered. The obtained results showed the feasibility of imposing limits to the orbit correction rate to a minimal value of, at least, one per day, as seen by the Fig. 8. Emphasis shall be given on the fact that this result was attained by considering the simulation of the autonomously generated coarse GPS navigation solution, instead of a more accurate system. The rate of generation of these estimates could be reduced from 1 estimates set each 10 seconds to one set each minute. The work can, yet, be complemented in future investigation in order to find the lower limit values of both the navigator estimates generation and maneuver application rates.

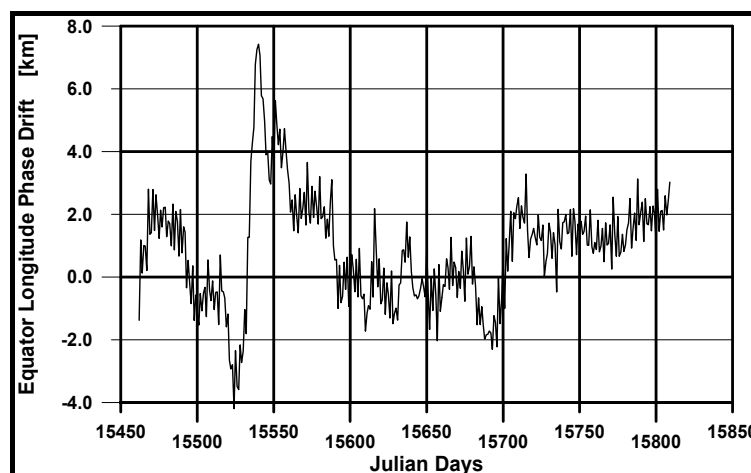


Fig. 8: Minimum Allowable Maneuver Rate of 1 Correction each 24 hours

The Fig. 9 shows superimposed on the same graphics, the curves of the estimated second derivative of ΔL_0 ($\ddot{\Delta L}$) and of the simulated solar flux as functions of time. The curve of $\ddot{\Delta L}(t)$, as one can observe from the figure, follows the shape of the average solar flux time variation, since it directly depends on the solar activity. One can see that the before mentioned inference of the level of the solar activity from the $\ddot{\Delta L}(t)$ estimates, in which the autonomous control procedure of adaptive discrete corrections amplitude is based, presented a effectively adequate characteristics to perform this task.

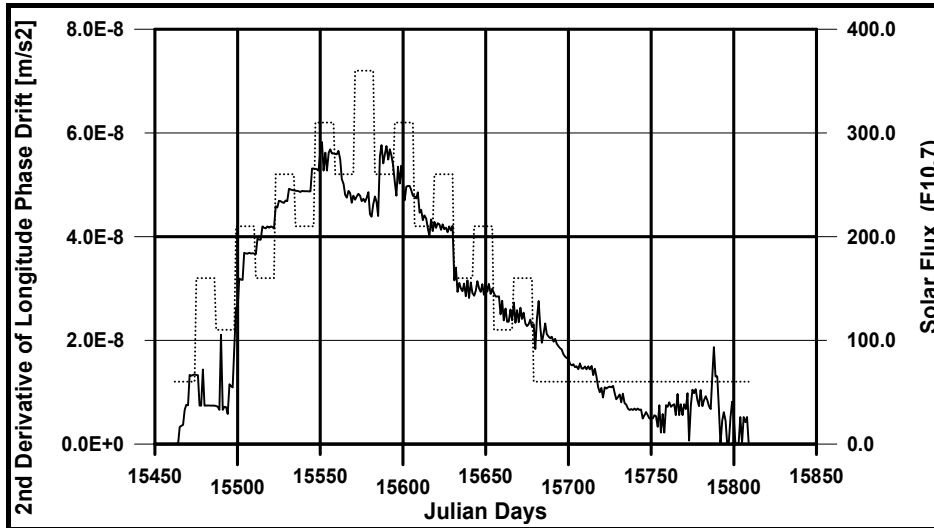


Fig. 9: Estimated Second Derivative of ΔL_0 and Simulated Solar flux

USE OF A SIMPLIFIED GPS NAVIGATOR

Complementing the studies, the use of a simplified GPS navigator, in order to supply the needed autonomous orbit observations (instead of the direct use of the GPS navigation solution) has been analyzed. Orbit simulation of the China-Brazil Earth Resources Satellite was used for this analysis. The idea behind using a simplified navigator was to allow the computation of improved orbit estimates from the position coordinates of the GPS (geometric) navigation solution, without adding a significant computational burden to the autonomous orbit control procedure. The bias in these coordinates, modeled as stochastic processes, were added the orbit dynamic equations. The Extended Kalman Filter was then applied to this increased dimension system, in order to estimate the observation bias components together with the orbit state vector. The main feature of this process is to automatically compensate for the effect of observation bias on the computed orbit state estimates.

In the propagation phase of the Kalman filter it was used a simplified orbit model that just includes the development of force due to the geopotential, considering spherical harmonics only until the zonal coefficient J_2 . In vector form the considered orbit dynamic model was the following:

$$\dot{\mathbf{x}}(t) = \mathbf{f}[\mathbf{x}(t), t] + \mathbf{G}(t) \boldsymbol{\omega}(t) \quad (16)$$

where: $\mathbf{x}(t) = [x_1(t) \ x_2(t) \ x_3(t) \ x_4(t) \ x_5(t) \ x_6(t)]^T$ is the orbit state vector; composed by the position (x_1, x_2, x_3) and velocity (x_4, x_5, x_6) components; $[\cdot]^T$ means the transpose of the related vector or matrix; $\mathbf{f}[\mathbf{x}(t), t]$ is a 6th dimension vector of non-linear functions of the orbital state; $\mathbf{G}(t)$ is a continuous 6x3 matrix; $\boldsymbol{\omega}(t)$ is a 3rd dimension vector which represents the uncertainties in the

knowledge of the forces acting on the satellite. It was assumed to be composed of gaussian white noise, with zero mean and matrix of spectral power density $\mathbf{Q}(t)$. The $\mathbf{G}(t)$ matrix is of the form:

$$\mathbf{G} = [0_{3 \times 3} \quad \mathbf{I}_{3 \times 3}]^T \quad (17)$$

Only the position coordinates of the coarse solution supplied by GPS receivers was used as observations for the Kalman filtering process, disregarding the less accurate velocity coordinates. The observation vector in the instant t_{k+1} was modeled as:

$$\mathbf{y}(t_{k+1}) = \mathbf{H} \mathbf{x}(t_{k+1}) + \mathbf{e}(t_{k+1}) + \mathbf{v}(t_{k+1}) \quad (18)$$

where $\mathbf{H} = [\mathbf{I}_{3 \times 3} \quad \mathbf{0}_{3 \times 3}]$, $\mathbf{e}(t_{k+1})$ is a 3rd dimension vector of the observation bias; $\mathbf{v}(t_{k+1})$ is 3rd dimension vector of random errors, assumed to be gaussian white noise with zero mean and covariance matrix given by the 3x3 matrix $\mathbf{R}(t_{k+1})$.

The bias of the GPS observations (on position components of the GPS coarse navigation solution), as commented previously, change their values whenever changes the set of GPS satellites which are used by the GPS receiver. They stay constant for periods between 1 to 15 minutes. Whenever a GPS satellite leaves or enters the receiver visibility region, a change in the bias values occurs. To take into account these observation bias variations, the following modeling was considered for the bias vector:

$$\mathbf{e}(t) = \boldsymbol{\omega}_e(t) \quad (19)$$

where $\boldsymbol{\omega}_e(t)$ is a 3rd dimension vector, which represents the uncertainty in the adopted observation bias model. It is supposed that $\boldsymbol{\omega}_e(t)$ follows a Gaussian distribution with zero mean and covariance matrix given by the 3x3 matrix \mathbf{Q}_e . The initial value $\mathbf{e}(t_0)$ is considered as a vector of gaussian random variables, with mean $\hat{\mathbf{e}}(t_0)$ and covariance matrix $\mathbf{P}_e(t_0)$, where $\hat{\mathbf{e}}(t_0)$ and $\mathbf{P}_e(t_0)$ are a priori estimates. It was assumed that $\mathbf{v}(t_k)$ is non-correlated with $\boldsymbol{\omega}_e(t)$ and $\hat{\mathbf{e}}(t_0)$.

By defining the following augmented system state vector:

$$\mathbf{x}_A(t) \equiv [\mathbf{x}(t) \quad \mathbf{e}(t)]^T, \quad (20)$$

and having in mind Equation 16, it follows that:

$$\dot{\mathbf{x}}_A(t) = \mathbf{f}_A[\mathbf{x}_A(t), t] + \mathbf{G}_A(t) \boldsymbol{\omega}(t), \quad (21)$$

where: $\mathbf{f}_A[\mathbf{x}_A(t), t] \equiv [\mathbf{f}_A[\mathbf{x}_A(t), t] \quad \mathbf{0}_{3 \times 1}]^T$; $\boldsymbol{\omega}_A(t) \equiv [\boldsymbol{\omega}(t) \quad \boldsymbol{\omega}_e(t)]^T$; and $\mathbf{G}_A \equiv \begin{bmatrix} \mathbf{G} & \mathbf{0}_{6 \times 3} \\ \mathbf{0}_{3 \times 3} & \mathbf{I}_{3 \times 3} \end{bmatrix}$.

Considering the definition of $\mathbf{x}_A(t)$, given by Equation 20 then, the Equation 18 can be put in the form:

$$\mathbf{y}(k+1) = \mathbf{H}_A \mathbf{x}_A(t_{k+1}) + \mathbf{v}(t_{k+1}) \quad (22)$$

where: $\mathbf{H}_A = [\mathbf{I}_{3 \times 3} \quad \mathbf{0}_{3 \times 3} \quad \mathbf{I}_{3 \times 3}]$. Considering the above definitions the error covariance matrix of the augmented state estimates and of dynamic system modeling takes the form:

$$\mathbf{Q}_A = \begin{bmatrix} \mathbf{Q}_{3 \times 3} & \mathbf{0}_{3 \times 3} \\ \mathbf{0}_{3 \times 3} & \mathbf{Q}_e_{3 \times 3} \end{bmatrix}; \quad \mathbf{P}_A = \begin{bmatrix} \mathbf{P}_{6 \times 6} & \mathbf{0}_{6 \times 3} \\ \mathbf{0}_{3 \times 6} & \mathbf{P}_e_{3 \times 3} \end{bmatrix}. \quad (23)$$

Applying the extended Kalman filter to the augmented system just defined, and accounting for the adopted assumptions, one has:

- **Time Update Phase:**

$$\hat{\mathbf{x}}_A(t_{k+1}/t_k) = \hat{\mathbf{x}}_A(t_k/t_k) + \int_{t_k}^{t_{k+1}} \mathbf{f}_A[\mathbf{x}_A(t), t] dt \quad (24)$$

$$\mathbf{P}_A(t_{k+1}/t_k) = \boldsymbol{\phi}_A[t_{k+1}/t_k; \hat{\mathbf{x}}_A(t_k/t_k)] \cdot \mathbf{P}_A(t_k/t_k) \cdot \boldsymbol{\phi}_A^T[t_{k+1}/t_k; \hat{\mathbf{x}}_A(t_k/t_k)] + \boldsymbol{\Gamma}_A(t_k) \cdot \mathbf{Q}_A(t_k) \cdot \boldsymbol{\Gamma}_A^T(t_k) \quad (25)$$

where:

$$\boldsymbol{\Gamma}_A(t_k) = \int_{t_k}^{t_{k+1}} \boldsymbol{\phi}_A[t_{k+1}, \tau] \mathbf{G}_A(\tau) d\tau, \quad \text{and} \quad \boldsymbol{\phi}_A[t_{k+1}/t_k; \hat{\mathbf{x}}_A(t_k/t_k)] = \begin{bmatrix} \boldsymbol{\phi}_{6 \times 6} & \mathbf{0}_{6 \times 3} \\ \mathbf{0}_{3 \times 6} & \mathbf{I}_{3 \times 3} \end{bmatrix} \quad (26)$$

- **Measurement Update Phase:**

$$\hat{\mathbf{x}}_A(t_{k+1}/t_{k+1}) = \hat{\mathbf{x}}_A(t_{k+1}/t_k) + \mathbf{K}[t_{k+1}; \hat{\mathbf{x}}_A(t_{k+1}/t_k)] \cdot \{ \mathbf{y}(t_{k+1}) - \mathbf{H}_A \hat{\mathbf{x}}_A(t_{k+1}/t_k) \} \quad (27)$$

$$\mathbf{P}_A(t_{k+1}/t_{k+1}) = \{ \mathbf{I} - \mathbf{K}[t_{k+1}; \hat{\mathbf{x}}_A(t_{k+1}/t_k)] \cdot \mathbf{H}_A \} \cdot \mathbf{P}_A(t_{k+1}/t_k) \quad (28)$$

where

$$\mathbf{K}[t_{k+1}; \hat{\mathbf{x}}_A(t_{k+1}/t_k)] = \mathbf{P}_A(t_{k+1}/t_k) \cdot \mathbf{H}_A^T \cdot \{ \mathbf{H}_A \cdot \mathbf{P}_A(t_{k+1}/t_k) \cdot \mathbf{H}_A^T + \mathbf{R}(t_{k+1}) \}^{-1} \quad (29)$$

Since the observation biases are estimated together with the satellite orbit state, their effects on the orbit estimates are automatically compensated for, improving, in this way, the estimates accuracy.

The simplified GPS navigator presented very satisfactory results in the performed simulation tests. It attained the prescribed objective of significantly improving the orbit estimates corresponding to the coarse GPS navigation solution. The existing systematic error in the position and velocity components of the GPS coarse solution was reduced by a factor of, respectively, the order of 60% and 85%. In addition, the developed autonomous navigator showed to have good robustness characteristic. In all performed long term simulations the Kalman filtering process did not present any divergence problem. It can, in this way, be concluded that the estimator re-initialization process (that was applied after each abrupt variation of the observation biases, that happens after each change of the set of visible GPS satellites) was very efficient in the task of avoiding filter divergence.

Further, the inclusion of the develop simplified navigator to the autonomous orbit control process was analyzed. Similarly to the previous studies, this analysis covered a period of about one-year, under unrealistically worse case conditions in terms of solar activity variation. Realistic (moderated) and critical conditions in terms of solar activities, shown in Fig. 10, were considered in this case.

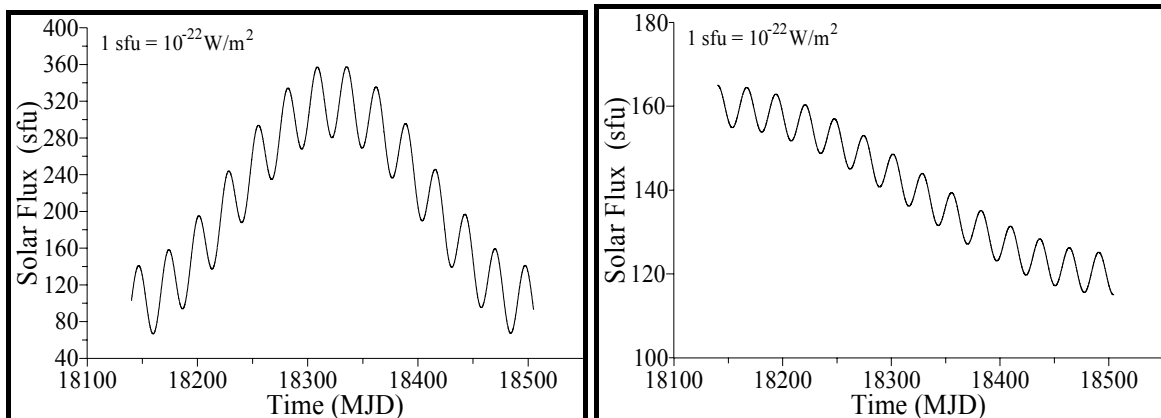


Fig. 10. Critical and Moderate Solar Activity Profiles

Even under worse case conditions in terms of solar activity, the autonomous control successfully maintained the Equator longitude phase drift ΔL_0 restricted to an excursion range of about -1000m

and 1700m. The introduction of the simplified navigator to the autonomous control procedure, successfully improved the control results, significantly reducing the variation range of ΔL_0 . Both realistic and worse case conditions in terms of solar activity were considered in the simulation. This study has been carried out considering the application of a version of the autonomous orbit control procedure, which considers only the application of semi-major axis corrections with a constant, previously chosen amplitude. Some improvements have, however, been implemented. In the original version the raw observation of both ΔL_0 and its first time derivative, $\dot{\Delta L}_0$, were computed from each simulated set of GPS orbit estimates. Now only the ΔL_0 observations are computed from the orbit estimates. The needed observations of $\dot{\Delta L}_0$ are directly computed, in a numerical way, from the last computed observations of ΔL_0 . Such approach increased the accuracy of the $\dot{\Delta L}_0$ observations and, as a consequence, the performance of the autonomous control process. A maximal maneuver application rate of about one pulse per orbit was considered. It was also considered a GPS observation rate (and consequently the navigator output rate) of 1 estimate each 9 seconds. Only one among 20 orbit estimates sets successively issued by the navigator is used by the control system.

The results considering the incorporation of the GPS simplified navigator to the autonomous control system, under critical solar activity condition, are shown in Fig. 11. The same observation rate above considered for the simplified navigator analysis was considered. Although the navigator supplies orbit estimates at a rate of 1 set each 9 seconds, the autonomous control procedure only used one of such sets each 9 minutes.

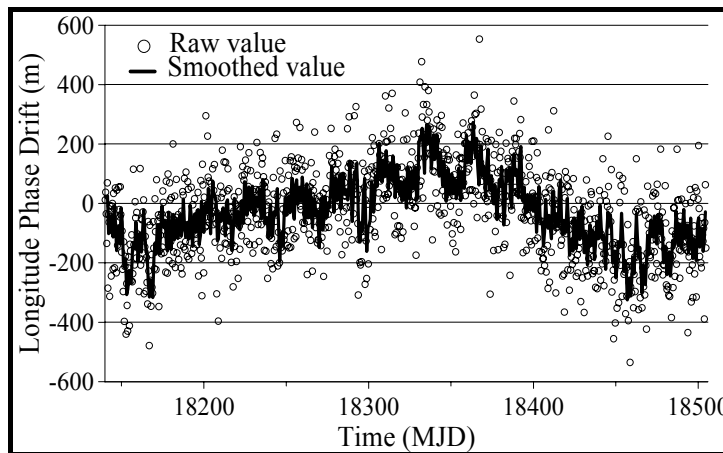


Fig. 11. Use of Simplified GPS Navigator (Critical Solar Activity Profile)

By comparing the results of the current investigation, depicted in Fig. 11, with the ones related to a previous analysis, presented above, one can see that the inclusion of the simplified navigator to the autonomous orbit control procedure produced a significant reduction in the variation range of ΔL_0 . The mean (smoothed) value of ΔL_0 remained in a range of about ± 300 m, which is about one order of magnitude lower than the previous case, where the coarse navigation solution was directly used in the autonomous control procedure. By improving the accuracy of the GPS coarse navigation solution, the use of the simplified navigator allowed, as expected, to obtain a consequent improvement of the autonomous control performance. The obtained results can be considered very promising. They reveal that a very relevant increment in the autonomous control accuracy can be obtained, with a relatively low increment in terms of the overall computational load imposed to the controller by the simplified navigator. In addition, these results indirectly show satisfactory robustness characteristics of the

simplified GPS navigator, since the accomplished tests considered, always, a long simulated period (about one year). It can be inferred from Fig. 11 that, during the entire simulated period, the navigator performed very conveniently, since any degradation occurred in the navigator performance would have no impact in the overall performance of the autonomous control system.

Fig. 12 presents the results obtained when moderate conditions in terms of solar activity were considered. All the other conditions cited in the case of the Fig. 11 were also been considered in the current one.

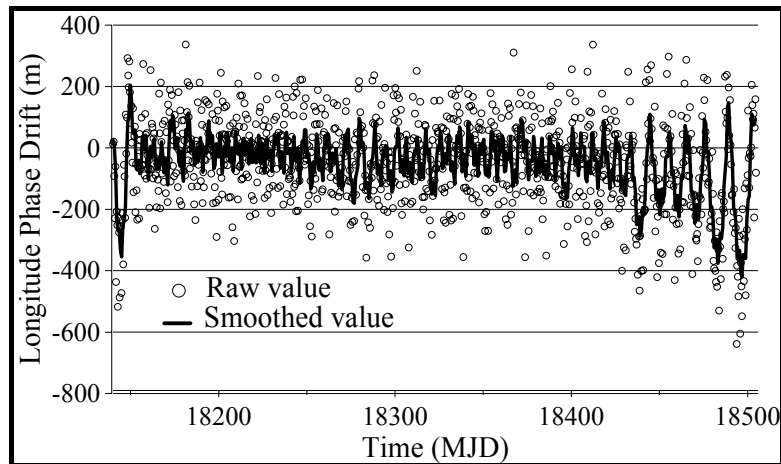


Fig. 12. Use of Simplified GPS Navigator (Moderate Solar Activity Profile)

We observe from Fig. 12 that the values of ΔL_0 remained in a variation range a little smaller than the one obtained under critical solar activity conditions (Fig. 11). The plot presents a behavior a little more stable than the one of Fig. 11. The increasing trend presented by the curve of Fig. 11, in the central region of the graphics, where the values of the critical solar flux conditions (Fig. 10) are higher, did not occur, as it could be expected, in the case of moderated solar activity condition.

CONCLUSIONS

The previous studies, considering a DIODE like navigator system as the source of autonomous orbit estimates, showed the feasibility of the autonomous orbit control concept. The results show a very satisfactory performance and good robustness characteristics, even under the worst case conditions considered in the tests. Further improvement, which consisted of the correction of the geopotential tesseral harmonics effects on the orbit inclination incremented the performance of the analyzed concept of autonomous control.

The investigation was then directed on the feasibility of using the autonomously generated GPS navigation solution, instead of a more accurate DIODE like orbit estimation. The results were very promising, since both types of developed autonomous control procedures have shown results which complied with the requirements imposed to the real Longitude phase drift control of existing satellites.

The analysis of the influence on the autonomous control procedure performance of the maximal allowable maneuver application rate showed the feasibility of imposing limits to the orbit correction rate to a maximal value of, at least, one per day. It shall be given emphasis on the fact that this result was attained by considering the simulation of the autonomously generated coarse GPS navigation solution, instead of a more accurate system. The rate of generation of these estimates was reduced from 1 estimates set each 10 seconds to one set each minute.

Finally, the use in the control procedure of a simplified GPS navigator, instead of the direct use of the GPS navigation solution has been analyzed. As expected, the use of more accurate orbit estimates in the computation of the needed observations of ΔL_0 improved the performance of the autonomous orbit control. Even under worse case conditions, in terms of solar activity, the longitude phase drift was maintained by the controller inside a reduced range of $\pm 300\text{m}$. This represents a relevant gain in terms of accuracy when compared with the results of a previous work, where the coarse GPS navigation solution was directly applied in the orbit control process. Another positive aspect which must be mentioned is that, due to the navigator simplicity, the obtained gain in terms of autonomous control performance did not imply in a prohibitive rise to the computer processing burden.

Although all the studies performed at INPE have always been done with help of simulated data, the obtained results showed the technical feasibility of a further autonomous orbit control application to a real satellite.

REFERENCES

- ***Berthias, J. P., Jayles, C.; Pradines, D.** "DIODE: a DORIS Based Real-time on-board Orbit Determination System for SPOT4", AAS/GSFC International Symposium on Spacecraft Ground Control and Flight Dynamics, 1993, Greenbelt, USA, pp. 125-138.
- ***Eckstein, M. C. ; Hechler, F.** "A Reliable Derivation of the Perturbations Due to Any Zonal and Tesseral Harmonics of the Geopotential for Nearly-circular Satellite Orbits", European Space Research Organization, ESRO SR-13, 1970.
- ***Galski, R. L.; Orlando, V.; Kuga, H. K.** "Autonomous Orbit Control Procedure, Using a Simplified GPS Navigator, Applied to the CBERS Satellite", International Symposium on Space Flight Dynamics, USA, 2002.
- ***Gill, E.** " Orbit Determination of the MIR Space Station from GPS Navigation Data, 12th Int. Symposium on Space Flight Dynamics, Darmstadt, Germany, 1997, pp. 41-48.
- ***R.C. Hart, S. Truong, A.C. Long,, T. Lee, J. Chan, D.H. Oza,** "GPS Navigation Initiatives at Goddard Space Flight Center Flight Dynamics Division", *Advances in the Astronautical Sciences, American Astronautical Society Publication*, Vol. 95, Part 1, 1997, pp. 315-327.
- ***Micheau, P.**"Orbit Control Techniques for Low Earth Orbiting Satellites", Space Flight Dynamics (chap. 13) course, CNES 1995, CEPADUES Editions.
- ***Noel, F.; Deleuze, M.; Laudet, P.; Valorge C.** "Operational Aspects of Precise Orbit Determination of SPOT and TOPEX/POSEIDON satellites with DORIS", AAS/GSFC Int. Symposium on Space Flight Dynamics, 1993, Greenbelt, USA, pp. 269.1-269.12.
- ***Orlando, V.; Kuga, H. K.** "Effect Analysis of the Maximal Allowable Maneuver Application Rate for an Autonomous Orbit Control Procedure Using GPS", 15th Int. Symposium on Space Flight Dynamics, 2000, Biarritz, France, pp. 143-148.
- ***Orlando V., Kuga, H. K.** "Analysis of an Autonomous Orbit Control Concept Using GPS", Journal of the Brazilian Society of Mechanical Sciences, Vol. XXI, Special Issue, 1999, pp. 52-59.
- ***Orlando, V.; Micheau, P.** "Autonomous Orbit Control System for Phased LEO Satellite" 11th IAS – Int. Astrodynamics Symposium, 1996, Gifu, Japan, pp. 143-148.

***Orlando, V.; Kuga, H. K.; Lopes, R. V. F.** “ Reducing the Geopotential Tesseral Harmonic Effects on Autonomous Longitude Drift Control of Sun-Synchronous Satellites”, “AAS Advances in the Astronautical Science”, AAS Publications Office, USA, 1997.

Tournier, T.; Berthias, J.; Jayles, C.; Mercier, F.; Laurichesse, D.; Cauquil, P.: "Orbit and Time On-Board Computation from the Current Spot4 Solution to Gns2 Needs", Journal of the Brazilian Society of Mechanical Sciences, Vol. XXI, Special Issue, February 1999, pp. 209-219.

***Putney, B.; Zelensky, N.; Klosko, S.** “TOPEX/POSEIDON Orbit Determination Production and Expert System”, Proceedings of the Second International Symposium on Ground Data Systems for Space missions operations, 1992, Pasadena, California, USA, pp. 585-590.